PPARγ controls cell proliferation and apoptosis in an RB-dependent manner

Lluis Fajas[1], Viviane Egler[1], Raphael Reiter[1], Stéphanie Miard[1], Anne-Marie Lefebvre[1] and Johan Auwerx*,[1]

[1]*Institut de Génétique et de Biologie Moléculaire et Cellulaire/CNRS/INSERM/ULP, 67404 Illkirch, France*

The nuclear receptor PPARγ is implicated in the control of cell proliferation and apoptosis. However, the molecular mechanisms by which it controls these processes remain largely elusive. We show here that PPARγ activation in the presence of the retinoblastoma protein (RB) results in the arrest of cells at the G1 phase of the cell cycle, whereas in the absence of RB, cells accumulate in G2/M, endoreduplicate, and undergo apoptosis. Through the use of HDAC inhibitors and coimmunoprecipitations, we furthermore demonstrate that the effects of RB on PPARγ-mediated control of the cell cycle and apoptosis depend on the recruitment of histone deacetylase 3 (HDAC3) to PPARγ. In combination, these data hence demonstrate that the effects of PPARγ on cell proliferation and apoptosis are dependent on the presence of an RB–HDAC3 complex.
Oncogene (2003) **22**, 4186–4193. doi:10.1038/sj.onc.1206530

Keywords: cancer; cell cycle; colon; nuclear receptor; transcription

Introduction

PPARγ is a nuclear receptor, initially characterized for its role in adipocyte differentiation, that can be activated by fatty acids or by synthetic agonists, such as the antidiabetic thiazolidinediones (reviewed in Rosen *et al.*, 2000). In addition to its role in metabolism, PPARγ has recently been implicated in the control of the cell cycle and apoptosis, and has been shown to be highly expressed in several human cancers (reviewed in Fajas *et al.*, 2001). Treatment of tumor cells with PPARγ agonists induced cell cycle arrest or stimulated apoptosis. In addition, small-scale clinical trials showed a reduction in tumor progression in patients with breast cancer, prostate cancer, or liposarcoma treated with thiazolidinediones (reviewed in Fajas *et al.*, 2001). Inhibition of E2F/DP DNA binding (Altiok *et al.*,

1997), induction of p21 (Morrison and Farmer, 1999), or downregulation of cyclin D1 expression (Wang *et al.*, 2001) have all been suggested as potential molecular mechanisms implicated in the control of cell cycle progression by PPARγ. In sharp contrast with this antitumor effect of PPARγ activation was the observation that PPARγ agonists induce tumor formation in APC-deficient mice (Lefebvre *et al.*, 1998; Saez *et al.*, 1998).

Little is known about the molecular mechanisms by which PPARγ agonists control cell proliferation and apoptosis. Since the retinoblastoma protein (RB) is a major regulator of these processes a crosstalk between PPARγ and RB signaling might exist. We recently described an interaction between PPARγ, RB and histone deacetylase 3 (HDAC3), which modulates PPARγ activity during adipocyte differentiation (Fajas *et al.*, 2002). RB controls cell growth, differentiation, and apoptosis via both E2F-dependent and -independent mechanisms (Hatakeyama and Weinberg, 1995). RB arrests cell proliferation through its interaction with the E2F family of transcription factors, which regulate the expression of genes involved in the progression into S phase, such as cyclin E (reviewed by Helin, 1998). Unphosphorylated RB binds to E2F and either blocks activation of E2F target genes or actively represses transcription through recruitment of HDACs (Brehm *et al.*, 1998; Magnaghi-Jaulin *et al.*, 1998). RB protects against apoptosis (Morgenbesser *et al.*, 1994; Pan and Griep, 1995), as demonstrated by widespread apoptosis in RB-deficient mice (Clarke *et al.*, 1992). This antiapoptotic effect of RB is mediated by inhibition of E2F1, as mutants for both RB and E2F1 show a reduction in apoptosis, indicating that the enhanced apoptosis in RB-deficient mice is mostly mediated by E2F1 (Tsai *et al.*, 1998).

We studied here the effects of PPARγ activation in different cells, which are defective for cell cycle regulators. We demonstrate that the capacity of PPARγ to promote cell cycle arrest, or apoptosis, depends on the RB status of the cell, suggesting that the interaction between both proteins also modulates PPARγ activity in the control of cell cycle and apoptosis. We furthermore suggest that the recruitment of HDAC3 to the PPARγ–RB complex contributes to these effects on cell cycle and apoptosis.

Results

### G1 arrest imposed by PPARγ activation is bypassed in the absence of RB

To test whether the ability of PPARγ to arrest cell proliferation was dependent on the expression of RB, mouse embryo fibroblasts (MEFs) derived from either RB+/+, or RB−/− mice, were treated for 48 h with the PPARγ agonist rosiglitazone and their cell cycle distribution analysed. Rosiglitazone arrested RB+/+ MEFs in G1 (Figure 1a). In contrast, rosiglitazone reduced the proportion of RB−/− MEFs in G1, and concomitantly stimulated their accumulation in G2/M and with more than $4N$ DNA content (Figure 1b). Giant and multinucleated cells were observed in rosiglitazone-treated RB−/− but not RB+/+ MEFs, indicating endoreduplication (Figure 1c, bottom panel). Under these conditions, rosiglitazone did not affect E2F activity directly (data not shown).

To demonstrate that these cell cycle effects were mediated by RB and PPARγ, two experiments were performed. First, when RB−/− MEFs were transfected with RB, RB−/− cells that expressed RB showed a cell cycle distribution resembling that of RB+/+ MEFs (compare Figure 1d and a). Second, no significant differences in cell cycle were observed upon rosiglitazone treatment of NIH-3T3 cells (Figure 1e), that did not express PPARγ (data not shown). When PPARγ was, however, ectopically expressed in these NIH-3T3 cells, rosiglitazone increased the proportion of cells in G1 (Figure 1f). To further demonstrate that PPARγ mediates the cell cycle arrest imposed by rosiglitazone, U2OS (RB+/+) cells were transfected with either a control or a PPARγ-specific siRNA labeled with fluorescein (6-FAM). This enabled us to identify, by fluorescence microscopy, cells which have incorporated the siRNA. Expression of PPARγ was not detected in green fluorescent cells (data not shown). No differences in BrdU incorporation in response to rosiglitazone were observed in these PPARγ-deficient U2OS cells, whereas a decrease in the number of BrdU positive cells was evident in cells transfected with the control siRNA and treated with rosiglitazone (Figure 1g). In combination, these data demonstrate that RB and PPARγ transduce the differential effects of rosiglitazone.

Gene expression is differentially regulated by rosiglitazone in RB+/+ or RB−/− cells

Consistent with accumulation of cells in G1, cyclin D3 and cyclin E decreased when RB+/+ cells were incubated with rosiglitazone (Figure 2a). Interestingly, expression of p27, a negative cell cycle regulator, was also slightly reduced by rosiglitazone in RB+/+ cells (Figure 2a), suggesting that downregulation of cyclin D3 and cyclin E is sufficient to block cell cycle progression. In sharp contrast with these results, rosiglitazone induced cyclin D3, cyclin E, and p27 expression in RB−/− cells (Figure 2a). Rosiglitazone did not affect PPARγ or actin protein levels (Figure 2a). Accumulation of these cyclins and p27 could explain endoreduplication in RB−/− cells in response to rosiglitazone.
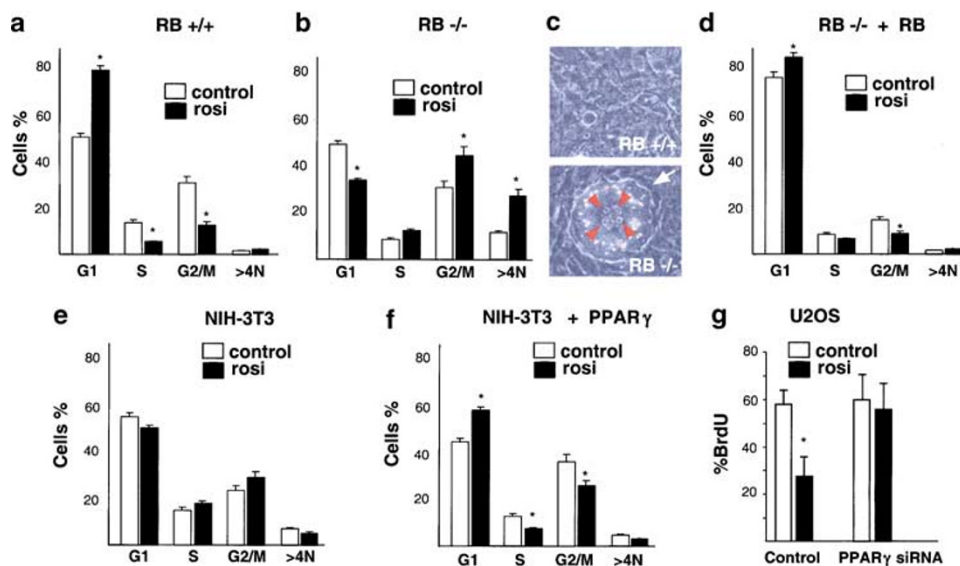
Figure 1 PPARγ regulation of the cell cycle in RB+/+ and RB−/− MEFs and in MIH-3T3 cells (**a**, **b**, **d**, **e**, **f**) FACS analysis of propidium iodide-stained cells comparing the cell cycle profile of asynchronously growing RB+/+ MEFs (**a**), RB−/− MEFs (**b**), RB−/− MEFs transfected with an RB expression vector (**d**), NIH-3T3 cells (**e**), or NIH-3T3 cells transfected with a PPARγ expression vector (**f**), in the absence (control) or presence of 10^{-6} M rosiglitazone (rosi). The number of cells in each phase of the cell cycle are quantified. Significant differences ($P < 0.05$ Student's t-test) are indicated by an asterisk. (**c**) Micrograph of rosiglitazone-treated RB+/+ MEFs and RB−/− MEFs under light microscopy (×30 magnification). The presence of a typical large endoreduplicating cell is indicated by an arrow. These cells contain several nuclei (arrowheads) and lipid droplets. (**g**) Quantification of BrdU incorporation analysed by immunofluorescence in U2OS cells transfected with either a control or a PPARγ-specific siRNA. Cells were stimulated with 10^{-6} M rosiglitazone. At least 500 cells were analysed
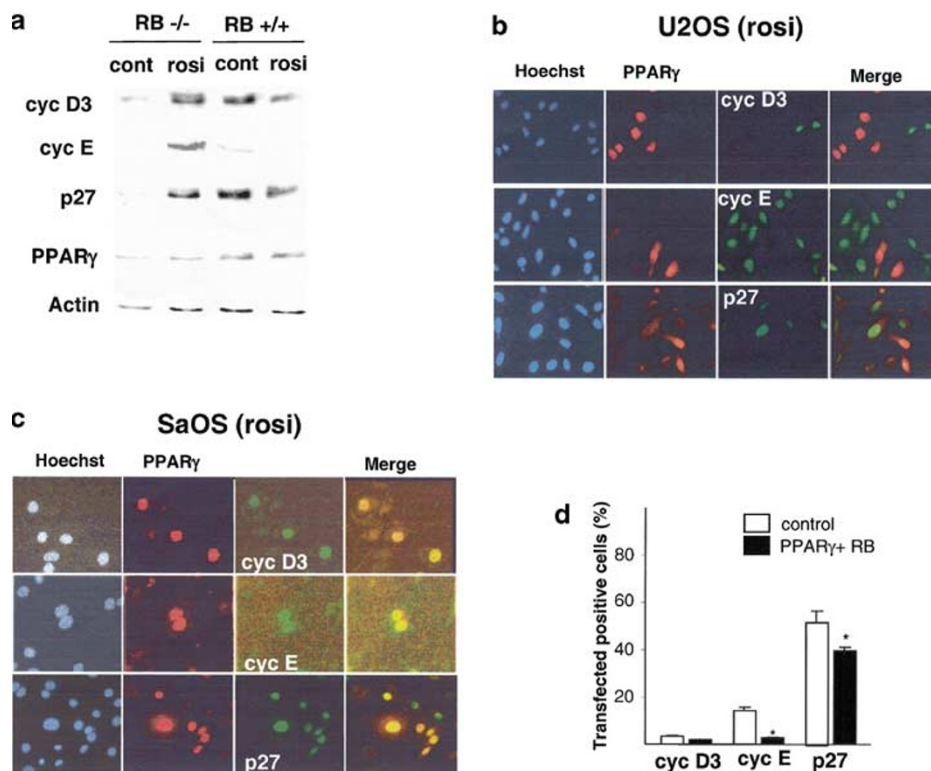
Figure 2 Effects of PPARγ on the expression of cell cycle regulated genes. (**a**) Western blot analysis showing the expression of cyclin D3 (cyc D3), cyclin E (cyc E), p27, PPARγ, and actin in RB−/− or RB+/+ MEFs incubated in the presence (rosi) or absence (cont) of 10^{-6} M rosiglitazone for 48 h. (**b**, **c**) Immunofluorescence analysis of U2OS (**b**) or SaOS (**c**) cells transfected with a PPARγ expression vector and exposed to 10^{-6} M rosiglitazone for 48 h. PPARγ-expressing cells are labeled in red, whereas cyclin D3, p27, or cyclin E proteins are stained in green. The merge panel shows colocalization of PPARγ with the tested proteins. Hoechst staining of nuclei (blue) is shown as control. (**d**) Quantification of the number of cells coexpressing PPARγ and the indicated proteins in SaOS cells transfected with either an RB expression vector (control) or PPARγ in combination with RB (PPARγ + RB). Cells were treated for 48 h with 10^{-6} M rosiglitazone

To further demonstrate that the differences in gene expression were directly related to PPARγ, either U2OS (RB+/+) or SaOS (RB−/−) cells were transfected with a PPARγ expression vector and treated for 24 h with rosiglitazone. Immunofluorescence analysis indicated that most of the U2OS cells transfected with PPARγ, did not express cyclin D3, cyclin E, or p27 (Figure 2b). In contrast, SaOS cells transfected with PPARγ, expressed more often cyclin D3, cyclin E, and p27 (Figure 2c). Furthermore, when SaOS cells were cotransfected with PPARγ and RB, the number of cells that express these cell cycle regulators decreased (Figure 2d). No effects were observed when a GFP-expressing vector was used instead of PPARγ (data not shown). Altogether, these results suggest that PPARγ regulates the expression of cell cycle-related genes in an RB-dependent manner.

PPARγ-mediated apoptosis is enhanced in the absence of RB

Next, we determined the effect of RB on PPARγ-mediated apoptosis in RB+/+ or RB−/− MEFs. Whereas no increase in apoptosis was observed in RB+/+ MEFs, a significant proportion of RB−/− MEFs underwent apoptosis when treated with rosiglitazone (Figure 3a and b). Similar results were obtained when the RB- and p53-deficient SaOS cells were compared to U2OS cells, indicating that the PPARγ-mediated apoptosis was p53-independent in the absence of RB (Figure 3b). Apoptosis was not induced with rosiglitazone, when RB expression was restored by transfecting an RB-expression vector in SaOS cells (Figure 3b). Furthermore, no increase in apoptosis was observed in rosiglitazone-treated SaOS cells in which PPARγ was inactivated by siRNA, demonstrating that the proapoptosis effects of rosiglitazone were mediated by PPARγ (Figure 3b).

To evaluate the effects of RB on PPARγ-mediated apoptosis under more physiological conditions, CaCo2 colon cells were differentiated and both PPARγ and total RB levels were evaluated by immunofluorescence. Between days 1 and 7 of differentiation, PPARγ remained constant, whereas RB levels decreased to the detection limit (Figure 3c). In contrast to cells at day 1, when RB is highly expressed and cells were resistant to PPARγ-induced apoptosis (Figure 3c), a significant proportion of rosiglitazone-treated cells at day 7 underwent apoptosis (Figure 3c). Interestingly, at this stage, RB was almost undetectable. Our data in MEFs, U2OS, SaOS, and in differentiated CaCo2 cells hence all
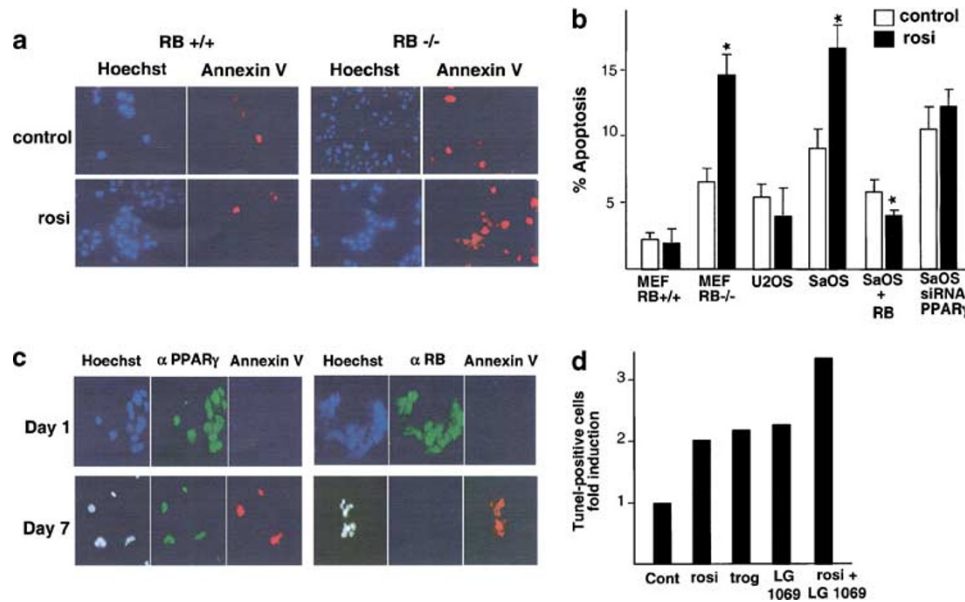
Figure 3 Effects of PPARγ on apoptotic events in RB−/− and RB+/+ MEFs. (**a**, **b**) Proliferating RB+/+ or RB−/− MEFs, U2OS, SaOS, SaOS cells transfected with RB, or SaOS cells transfected with a PPARγ-specific siRNA, were cultured in the presence (rosi) or absence (control) of 10^{-6} M rosiglitazone for 3 days. Cells were harvested and incubated with the apoptosis marker Annexin V, and labeled with a red fluorochrome. At least 500 cells were analysed for Annexin V. Statistically significant differences ($P < 0.05$; Student's *t*-test) are indicated. (**c**) Fluorescence micrograph of post-confluent (day 1) or differentiated (day 7) CaCo2 cells exposed to rosiglitazone for 3 days. Cells were harvested and incubated with a red fluorochrome-labeled Annexin V together with anti-PPARγ (α PPARγ) or an anti-RB (α RB) antibody. Incubation of the cells with FITC-labeled secondary antibody (green labeling) was used to detect the presence of PPARγ or RB. (**d**) Evaluation of apoptosis by TUNEL assay in differentiated HT-29 cells after 3 days treatment with DMSO (Cont), troglitazone (trog), rosiglitazone (rosi), the rexinoid LG1069 or both agents combined (rosi+LG1069). Each compound was at a final concentration of 10^{-6} M. The results are indicated as fold-induction compared to DMSO

support our hypothesis that PPARγ-mediated apoptosis is dependent on RB.

Also in another colon cell line, that is, the HT-29 cell line, which does not contain functional p53, rosiglitazone and troglitazone induced apoptosis as measured by terminal deoxynucleotidyl transferase-mediated dUTP nick-end labeling (TUNEL) activity (Figure 3d). Similar to CaCo2 cells, expression of RB was decreased, whereas PPARγ was induced upon differentiation of HT-29 cells (Lefebvre *et al.*, 1999). Additional TUNEL assays demonstrated that the RXR agonist LGD1069 induced apoptosis in differentiated HT-29 cells to the same extent as rosiglitazone or troglitazone (Figure 3d), whereas the combination of both PPARγ and RXR agonists was more effective in inducing apoptosis, relative to each compound alone (Figure 3d). The fact that both RXR and PPARγ agonists induced apoptosis was supportive of the involvement of the RXR/PPARγ heterodimer.

Apoptosis induced by PPARγ agonists was also evaluated by TUNEL assays in 3T3-L1 cells before and after differentiation into adipocytes. Rosiglitazone and troglitazone did not affect apoptosis in undifferentiated 3T3-L1 cells (Figure 4a). In contrast, in differentiated 3T3-L1 adipocytes, both agonists induced TUNEL-positive cells (Figure 4a). This effect was dependent on the dose of rosiglitazone (Figure 4b, and data not shown). PPARγ protein was highly expressed in these differentiated adipocytes, and although RB was expressed, it was to a significant extent hyperpho-

sphorylated, and thus inactive (Figure 4c). Phosphorylation of RB was verified by the disappearance of the slower migrating band upon alkaline phosphatase treatment of the nuclear extracts (data not shown). Consistent with the presence of phosphorylated RB, cyclin D3 was also induced (Figure 4c). These results suggest that PPARγ activation, in the presence of inactive RB, promotes apoptosis in differentiated 3T3-L1 adipocytes, but is unable to do so in undifferentiated 3T3-L1 cells, when the ratio of RB/phosphorylated RB is high and PPARγ levels are low. Interestingly, cell cycle analysis of 3T3-L1 cells either before (confluent) or 6 days after induction of differentiation indicated that cells at day 6 accumulated in G2/M and often had a DNA content $>4N$ (Figure 4d, upper panel), a situation reminiscent of rosiglitazone-treated RB−/− MEFs (Figure 1b). The lack of BrdU incorporation in these cells indicated cell cycle arrest (data not shown), whereas the induction of aP2 mRNA (Figure 4d, lower panel), an adipocyte marker, proved that cells at day 6 were actually differentiated.

Inhibition of HDAC activity restores PPARγ transcriptional activation

To evaluate the influence of RB on PPARγ activation, transient cotransfection experiments were performed in RB−/− MEFs using a PPARγ-responsive luciferase reporter. A 2.5-fold induction of PPARγ-induced luciferase activity was observed in the presence of
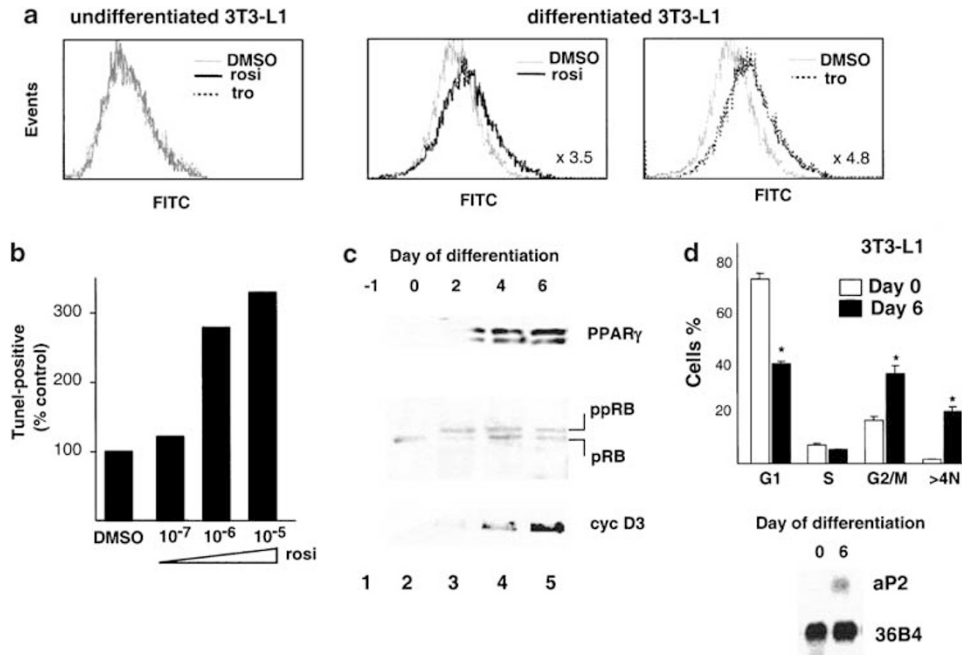
Figure 4 PPARγ-mediated apoptosis in 3T3-L1 adipocytes. (**a**) Apoptosis events evaluated by TUNEL assay in undifferentiated cells or differentiated 3T3-L1 cells. Assays were done 3 days after treatment with either vehicle alone (DMSO), rosiglitazone (rosi) or troglitazone (trog), both at a final concentration of 10^{-6} M. The histograms depict fluorescence (FITC) intensity per cell on the *x*-axis and the number of cells on the *y*-axis (events). Increase in fluorescence correlates with increased apoptosis, indicated as fold induction in the right bottom corner. (**b**) Quantification of apoptosis by TUNEL in differentiated 3T3-L1 cells treated for 3 days with rosiglitazone. The amount of apoptosis correlates with the concentration of rosiglitazone. (**c**) Western blot of PPARγ, RB, and cyclin D3, during 3T3-L1 differentiation. Phosphorylated RB (ppRB) is the slower migrating band relative to hypophosphorylated RB (pRB). (**d**) Cell cycle profile of 3T3-L1 cells at confluence (day 0), or at day 6 of differentiation. Differentiation of the cells at day 6 was demonstrated by the increased expression of aP2 mRNA in Northern blot hybridization

rosiglitazone. This induction was significantly attenuated by cotransfection of RB (Figure 5a), suggesting that RB is a corepressor factor of PPARγ. Since repression of gene transcription by RB is usually mediated by recruitment of HDACs (Brehm *et al.*, 1998; Fajas *et al.*, 2002), it could be possible that this was the mechanism by which RB represses PPARγ-mediated transcription. To prove that the attenuation of PPARγ activity in the presence of RB was mediated by HDACs, a cotransfection experiment was performed in the presence of the HDAC inhibitor trichostatin A (TSA). Incubation of the RB−/− cells with rosiglitazone induced luciferase activity of the PPARγ-responsive promoter about 1.5-fold, in the presence of transfected RB. This effect was increased 3.5-fold when cells were incubated with both rosiglitazone and TSA (Figure 5a), suggesting that TSA released PPARγ from the RB–HDAC repressor complex. Consistent with this, was the fact that TSA had no synergistic effect with rosiglitazone in the absence of RB (Figure 5a). Addition of TSA alone had no effect on PPARγ activation (Figure 5a). Similar results were obtained with sodium butyrate (data not shown). No differences in β-gal activity were observed indicating that the TSA effects were specific. These results suggested that inhibition of HDAC could abrogate the repressive effects of RB on PPARγ activity.

Next, we analysed the effects of HDAC inhibition on the changes in cell cycle distribution of the RB+/+ U2OS cells in response to rosiglitazone. Incubation with TSA resulted in the accumulation of the U2OS cells in G2/M (Figure 5c). This effect of TSA was enhanced when rosiglitazone was added (Figure 5c). This result in TSA-treated U2OS cells is similar to the cell cycle profile seen after activation of PPARγ in RB−/− cells (Figure 1b), and further proves that the repressive effects of RB on PPARγ activity are mediated by HDACs.

The expression of cyclin D3, cyclin E, and p27 was next analysed by immunofluorescence in U2OS cells transfected with PPARγ. Rosiglitazone treatment resulted in a decrease in the number of cells expressing either cyclin D3, cyclin E, or p27 (Figure 5d). In contrast, when TSA and rosiglitazone were combined, a robust increase in the number of PPARγ-transfected cells expressing either cyclin D3, cyclin E, or p27 was observed. This increase was similar to that observed in RB−/− cells treated with rosiglitazone (Figure 2c), suggesting that HDAC inhibition disrupts the activity of PPARγ–RB–HDAC3 repressor complex.

Finally, the presence of a PPARγ–RB–HDAC protein complex in U2OS cells was analysed by coimmunoprecipitation studies. Consistent with our previous results in the context of adipocyte differentiation (Fajas *et al.*, 2002), we found that both RB and HDAC3 imunoprecipitated with PPARγ in U2OS cells (Figure 5d).
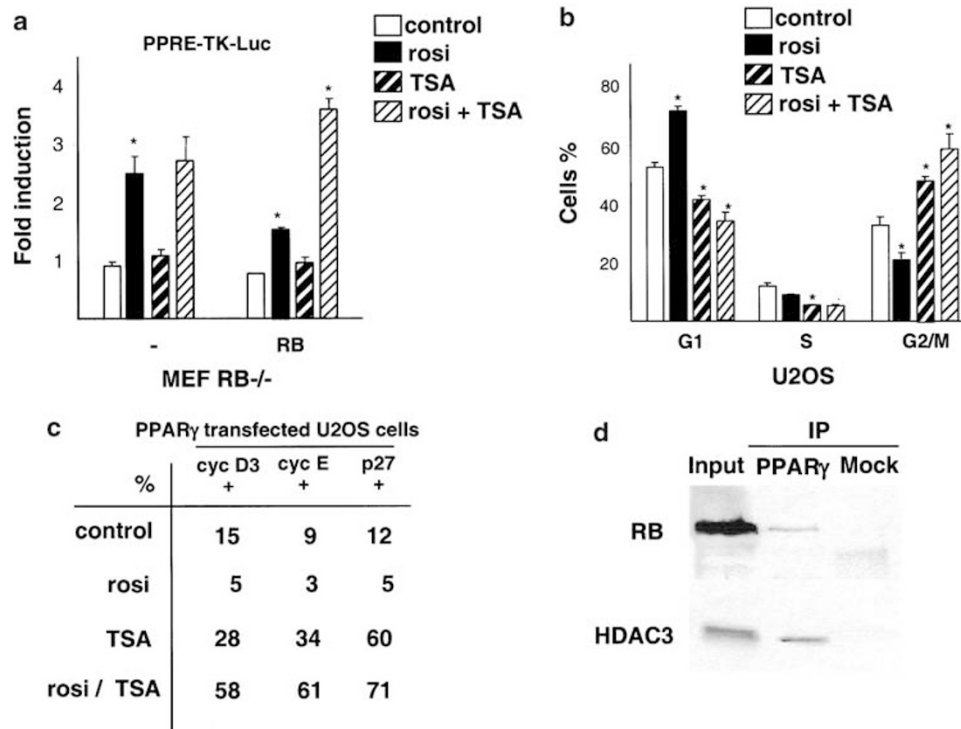
Figure 5 PPARγ activity is restored in RB+/+ cells in the presence of HDAC inhibitors. (**a**) Luciferase activity generated from a PPRE-driven luciferase reporter vector (PPRE-TK-Luc) cotransfected in RB−/− MEFs with either a control or an expression vector for RB. The experiments were performed in the presence of either vehicle (control), 10^{-6} M of rosiglitazone (rosi), 10^{-7} M of trichostatin A (TSA), or a combination of rosiglitazone and trichostatin A (rosi + TSA). Fold induction of reporter activity by rosiglitazone treatment relative to control is indicated. The concentration of compounds is the same in all subsequent panels of Figure 5. Significant differences ($P < 0.05$ Student's t-test) are indicated by an asterisk in panels a–c. (**b**) FACS analysis of propidium iodide stained U2OS cells comparing the cell cycle profile of asynchronously growing cells treated with rosiglitazone, TSA, or a combination of both. The number of cells in each phase of the cell cycle are quantified. Significant differences from control ($P < 0.05$ Student's t-test) are indicated by an asterisk. (**c**) Quantification of the number of PPARγ-transfected U2OS cells treated with vehicle (control), rosiglitazone, TSA, or a combination of both that coexpress PPARγ and either cyclin D3, cyclin E, or p27, measured by immunofluorescence assays. At least 300 cells were quantified. Numbers are percentage of PPARγ-expressing cells. (**d**) Immunoprecipitation assay showing interaction between HDAC3, RB, and PPARγ. Extracts from U2OS cells were immunoprecipitated with anti-PPARγ (lane 2), preimmune serum (Mock, lane 3), or directly analysed for the presence of RB, or HDAC3 (input, lane 1). Western blot analysis revealed the presence of RB (upper panel), or HDAC3 (lower panel) in PPARγ immunoprecipitates

Discussion

Little is known about the molecular mechanisms by which PPARγ ligands control cell proliferation and apoptosis. Since RB has been implicated in the same physiological events, we postulated that RB and PPARγ signaling pathways might interact and together control the cell cycle and apoptosis. Such a hypothesis would, furthermore, be consistent with our recent observation that the formation of an RB–PPARγ complex also represses PPARγ signaling during adipocyte differentiation (Fajas et al., 2002).

RB and HDAC3 change the activity of PPARγ in the control of the cell cycle

Depending on the RB status of the cell, differential effects of PPARγ on the cell cycle are observed. MEFs, where both PPARγ and RB proteins are present, are arrested in G1 upon treatment with PPARγ activators, as has been described for other cell types (Altiok et al.,

1997; Chang and Szabo, 2000; Wakino et al., 2000; Koga et al., 2001; Wang et al., 2001). The activity of PPARγ in the control of the cell cycle is, however, changed in the absence of RB, since both RB−/− MEF and RB-deficient SaOS cells escape from the PPARγ imposed G1 arrest, and accumulate in G2/M; a significant number of these cells also endoreduplicate. Furthermore, rescue of RB expression in RB−/− cells restores G1 arrest of the cell cycle in response to PPARγ agonists. The involvement of HDACs in mediating the effects of PPARγ–RB on these cell cycle parameters was suggested by the fact that the cell cycle profile and the expression of cyclin D3 and E of RB+/+ U2OS cells, treated with HDAC inhibitors, resembled to that of rosiglitazone-treated RB−/− MEFs. Moreover, in coimmunoprecipitation studies we provide evidence that PPARγ interacts with both RB and HDAC3 in U2OS cells, a phenomenon similar to the PPARγ–RB–HDAC3 complex we described recently in adipocytes (Fajas et al., 2002). Interestingly, a recent report showed that HDAC inhibitors were more effective in supressing

growth and inducing differentiation of lung adenocarcinoma cells when used in combination with PPARγ agonists (Chang and Szabo, 2002).

RB might attenuate PPARγ activation, as we have shown in transient transfection studies, and hence decrease the expression of the cell cycle regulators cyclin D3, cyclin E, and p27. Again HDACs might mediate the attenuation of the expression of these cell cycle regulators by RB, since HDAC inhibition can overcome this effect. Although it has not yet been shown that cyclin D3 and cyclin E are direct targets for PPARγ, their lower expression levels upon rosiglitazone treatment in RB+/+ relative to RB−/− cells could be explained by inhibition of PPARγ activity by RB, and hence underlie the G1 arrest in RB+/+ cells. In addition, in the absence of active RB, PPARγ could more effectively stimulate the expression of the negative cell cycle regulators, p21 or p27. Consistent with this, p27 was increased in RB−/− cells in response to PPARγ activation. Increased expression of p21 or p27 in the absence of RB favors cell cycle arrest in G2/M and endoreduplication (Niculescu et al., 1998; Chang et al., 2000), similar to the situation in rosiglitazone-treated RB−/− MEFs.

Some of these results seem apparently at odds with previous studies of PPARγ agonists in RB-negative cells (Koga et al., 2001; Wang et al., 2001). Differences in the experimental design are most likely responsible for these discrepancies. Repression of the cyclin D1 promoter by PPARγ has been shown in RB-deficient HeLa cells (Wang et al., 2001). However, PPARγ-mediated repression of the cyclin D1 promoter in these cells was mediated by competition between the activating protein 1 (AP1) and PPARγ for binding to the transcriptional coactivator p300 and did not involve RB. Troglitazone also induced a G1 arrest in HLF hepatoma cells, which do not express RB (Koga et al., 2001). These last studies were performed, however, in the presence of high concentrations of troglitazone (50 μM). This concentration is 50-fold higher than the concentration of rosiglitazone that was used in the present study. In addition, troglitazone has been shown to have significant PPARγ-independent effects in the control of cell cycle (Palakurthi et al., 2001).

PPARγ, RB, and apoptosis

Whereas activation of PPARγ induces apoptosis (Elstner et al., 1998; Padilla et al., 2000), RB has been demonstrated to have an antiapoptotic function (Morgenbesser et al., 1994; Pan and Griep, 1995). This is consistent with our finding that in the absence of RB, PPARγ-mediated apoptosis is enhanced. Two hypotheses, which are not mutually exclusive, could explain an effect of RB on PPARγ-mediated apoptosis. *First*, whereas in the absence of RB, PPARγ might directly stimulate the expression of some apoptosis-related genes such as Bax, this stimulation might be attenuated in the presence of RB. *Second*, apoptosis imposed by PPARγ in RB−/− cells could merely be the consequence of the G2/M arrest or endoreduplication, that are both

conditions that favour apoptosis. Most interesting is our observation that activation of PPARγ in differentiated colon cells, where RB is almost absent, induces apoptosis. This mimics the *in vivo* situation, since PPARγ is strongly expressed (Lefebvre et al., 1999) and RB is almost absent (Guy et al., 2001; Yamamoto et al., 1999) in differentiated epithelial cells found at the top of the villi in the colon. One of the consequences of the high ratio of PPARγ to RB expression in the villi is the stimulation of apoptosis, which contributes to cell turn-over in normal colon.

In summary, we have shown that, similar to their role in the control of the transcription factor E2F1, RB and HDACs inhibit PPARγ activity, through a direct interaction, thereby modulating its effects on the cell cycle and apoptosis. This supports the concept that RB and HDAC3 are general modulators of PPARγ activity in many physiological systems with a direct impact on PPARγ effects on cell cycle control, apoptosis (this study), and differentiation (Fajas et al., 2002).

Materials and methods

Materials

Rosiglitazone, troglitazone, and LGD 1069 were kind gifts of Dr R Heyman of X-ceptor pharmaceuticals (San Diego, CA, USA). All chemicals, except if stated otherwise, were purchased from Sigma (St Louis, MO, USA). Anti-PPARγ (E-8), anti-cyclin E (M-20), anti-cyclin D3 (D-7), anti-actin (sc1616), and anti-p27 (F-8) antibodies were purchased from Santa Cruz Biotechnology (Santa Cruz, CA, USA). The anti-RB antibody (G3-245) was purchased from Pharmingen (San Diego, CA, USA).

Plasmids, proteins, and siRNAs

PPARγ and RB expression vectors, and the PPARγ-responsive luciferase reporter constructs were all described in detail previously (Fajas et al., 1997, 2000). The pEGFP vector was purchased from Promega (Charbonnières, France). PPARγ-specific fluorescein-labeled siRNA was synthesized by Xeragon (Germantown, MD USA). The sequence of the oligoribonucleotide was 5′ GCCCUUCACUACUGUUGAC dTdT 3′.

Cell culture, protein extracts, and transfections

MEFs (a gift from Dr JM Blanchard), 3T3-L1, U2OS, and SaOS cells (ATCC, Manassas, VA, USA) were grown in DMEM with 10% fetal calf serum (FCS). Cells were differentiated with DMEM, 10% serum, and MDI (0.5 mM 3-isobutyl-1-methylxanthine (IBMX), 10 μg/ml insulin and 1 μM dexamethasone) was added in some experiments for 2 days. From day 3 on, cells were incubated with DMEM, 10% serum, 10 μg/ml insulin, and 10⁻⁶ M rosiglitazone when stated. Oil-red-O staining is described elsewhere (Rocchi et al., 2001). Human colon adenocarcinoma CaCo2 and HT-29 cells (ATCC) were grown in Mc Coy's medium supplemented with 10% FCS. Cells were rendered quiescent at confluency and treated with the different compounds. Nuclear and whole-cell extracts were prepared as described (Fajas et al., 1997). Transfections were performed using lipofectamine (Life Technologies, Rockville, MD, USA), and luciferase and β-gal activity was measured as described (Fajas et al., 1997).

Flow cytometry analysis, BrdU, and apoptosis assays

Proliferating RB+/+ or RB−/− MEFs were incubated with 10^{-6} M rosiglitazone for 2 days. Cells were harvested, fixed with 70% EtOH, and DNA was labeled with propidium iodide. Cells were sorted by FACS analysis (Coulter Electronics, Hialeah, FL, USA) and cell cycle profiles were determined using the ModFit software (Becton Dickinson, San Diego, CA, USA). Apoptotic cells were detected by Alexa 568 conjugated Annexin V labeling following instructions of the manufacturer (Roche, Meylan, France). For the terminal deoxynucleotidyl transferase-mediated dUTP nick-end labeling (TUNEL) procedure, we followed recommendations of the manufacturer (Roche). Quantification of the TUNEL assay was performed by FACS analysis. For BrdU incorporation, cells were incubated 4 h in the presence of BrdU and an additional treatment of the cells with 1.5 N HCl for 10 min at 21°C was performed after fixation as described below.

Western blot and Northern blot analysis

SDS–PAGE and electrotransfer was performed as described (Fajas *et al.*, 1997). The membranes were blocked overnight in blocking buffer (20 mM Tris, 100 mM NaCl, 1% Tween-20, 10% skim milk). Filters were first incubated 4 h at 21°C with primary antibody, and then for 1 h at 21°C with a peroxidase conjugate secondary antibody. The complex was visualized with 4-chloro-1-naphtol.

Immunofluorescence

For all immunofluorescence experiments, cells were grown on coverslips. After fixation and permeabilization with methanol, cells were incubated with antibodies. Preparations were then incubated with a combination of Texas Red-conjugated anti-mouse IgG and FITC-conjugated anti-rabbit IgG.

Immunoprecipitation

Coimmunoprecipitation assays were performed as previously described (Fajas *et al.*, 2002).

References

Altiok S, Xu M and Spiegelman B. (1997). *Gen. Dev.*, **11,** 1987–1998.

Brehm A, Miska EA, McCance DJ, Reid JL, Bannister AJ and Kouzarides T. (1998). *Nature*, **391,** 597–601.

Chang BD, Broude EV, Fang J, Kalinichenko TV, Abdryashitov R, Poole JC and Roninson IB. (2000). *Oncogene*, **19,** 2165–2170.

Chang TH and Szabo E. (2000). *Cancer Res.*, **60,** 1129–1138.

Chang TH and Szabo E. (2002). *Clin. Cancer Res.*, **8,** 1206–1212.

Clarke AR, Maandag ER, van Roon M, van der Lugt NM, van der Valk M, Hooper ML, Berns A and te Riele H. (1992). *Nature*, **359,** 328–330.

Elstner E, Muller C, Koshizuka K, Williamson EA, Park D, Asou H, Shintaku P, Said JW, Heber D and Koeffler HP. (1998). *Proc. Nat. Acad. Sci. USA*, **95,** 8806–8811.

Fajas L, Auboeuf D, Raspe E, Schoonjans K, Lefebvre AM, Saladin R, Najib J, Laville M, Fruchart JC, Deeb S, Vidal-Puig A, Flier J, Briggs MR, Staels B, Vidal H and Auwerx J. (1997). *J. Biol. Chem.*, **272,** 18779–18789.

Fajas L, Debril MB and Auwerx J. (2001). *J. Mol. Endocrinol.*, **27,** 1–9.

Fajas L, Egler V, Reiter R, Hansen J, Kristiansen K, Miard S and Auwerx J. (2002). *Dev. Cell*, **3,** 903–910.

Fajas L, Paul C, Zugasti O, Le Cam L, Polanowska J, Fabbrizio E, Medema R, Vignais ML and Sardet C. (2000). *Proc. Natl. Acad. Sci. USA*, **97,** 7738–7743.

Guy M, Moorghen M, Bond JA, Collard TJ, Paraskeva C and Williams AC. (2001). *Br. J. Cancer*, **84,** 520–528.

Hatakeyama M and Weinberg RA. (1995). *Prog. Cell Cycle Res.*, **1,** 9–19.

Helin K. (1998). *Curr. Opin. Genet. Dev.*, **8,** 28–35.

Koga H, Sakisaka S, Harada M, Takagi T, Hanada S, Taniguchi E, Kawaguchi T, Sasatomi K, Kimura R, Hashimoto O, Ueno T, Yano H, Kojiro M and Sata M. (2001). *Hepatology*, **33,** 1087–1097.

Lefebvre A, Chen I, Desreumaux P, Najib J, Fruchart J , Geboes K, Briggs M, Heyman R and Auwerx J. (1998). *Nat. Med.*, **4,** 1053–1057.

Lefebvre AM, Paulweber B, Fajas L, Woods J, McCrary C, Colombel J-F, Najib J, Fruchart J-C, Datz C, Vidal H, Desreumaux P and Auwerx J. (1999). *J. Endocrinol.*, **162,** 331–340.

Magnaghi-Jaulin L, Groisman R, Naguibneva L, Robin P, Lorain S, Le Villain JP, Troalen F, Trouche D and Harel-Bellan A. (1998). *Nature*, **391,** 601–605.

Morgenbesser SD, Williams BO, Jacks T and DePinho RA. (1994). *Nature*, **371,** 72–74.

Morrison RF and Farmer SR. (1999). *J. Biol. Chem.*, **274,** 17088–17097.

Niculescu III AB, Chen X, Smeets M, Hengst L, Prives C and Reed SI. (1998). *Mol. Cell. Biol.*, **18,** 629–643.

Padilla J, Kaur K, Cao HJ, Smith TJ and Phipps RP. (2000). *J. Immunol.*, **165,** 6941–6948.

Palakurthi SS, Aktas H, Grubissich LM, Mortensen RM and Halperin JA. (2001). *Cancer Res.*, **61,** 6213–6218.

Pan H and Griep AE. (1995). *Genes Dev.*, **9,** 2157–2169.

Rocchi S, Picard F, Vamecq J, Gelman L, Potier N, Zeyer D, Dubuquoy L, Bac P, Champy MF, Plunket KD, Leesnitzer LM, Blanchard SG, Desreumaux P, Moras D, Renaud JP and Auwerx J. (2001). *Mol. Cell*, **8,** 737–747.

Rosen ED, Walkey CJ, Puigserver P and Spiegelman BM. (2000). *Genes Dev.*, **14,** 1293–1307.

Saez E, Tontonoz P, Nelson MC, Alvarez JGA, Ming UT, Baird SM, Thomazy VA and Evans RM. (1998). *Nat. Med.*, **4,** 1058–1061.

Tsai KY, Hu Y, Macleod KF, Crowley D, Yamasaki L and Jacks T. (1998). *Mol. Cell*, **2,** 293–304.

Wakino S, Kintscher U, Kim S, Yin F, Hsueh WA and Law RE. (2000). *J. Biol. Chem.*, **275,** 22435–22441.

Wang C, Fu M, D'Amico M, Albanese C, Zhou JN, Brownlee M, Lisanti MP, Chatterjee VK, Lazar MA and Pestell RG. (2001). *Mol. Cell. Biol.*, **21,** 3057–3070.

Yamamoto H, Soh JW, Monden T, Klein MG, Zhang LM, Shirin H, Arber N, Tomita N, Schieren I, Stein CA and Weinstein IB. (1999). *Clin. Cancer Res.*, **5,** 1805–1815.